Modelling Heat Flow in a Heat Storage System with the Use of the Finite Volume Method

Wojciech Sobieski

Department of Mechanics and Machine Design
University of Warmia and Mazury in Olsztyn,
wojciech.sobieski@uwm.edu.pl

Abstract. *Non-stationary heat flow was analysed in a heat storage system comprising a flat multilayer structure with different parameters and thickness. Concrete was the heat storage material, and water was the transfer medium responsible for supplying and evacuating heat from the storage medium. It was assumed that the modelled heat storage system may be powered by a solar thermal collector. Data were collected over a period of 24 hours, and they were analysed separately for the heat accumulation phase and the heat recovery phase. Calculations were performed in a program developed by the author based on the Finite Volume Method (FVM). The main aim is to illustrate the basic features of the developed numerical code and to find effective methods for evaluating the applicability of the modelled structures for heat storage. Except that, in the paper the possibilities are discussed for the use of the source component of the diffusion equation to describe various phenomena of physical, chemical and biological nature. The present article was motivated by the observation that FVM is currently not applied in the process of designing heat storage systems.*

Keywords: *heat transfer, heat storage, multilayer wall, numerical modelling, Finite Volume Method.*

1. Introduction

Thermal energy storage, in particular long-term storage, is one of the greatest challenges in contemporary power systems supplied with renewable energy. According to research, various forms of energy can be derived from renewable resources; however, the energy supply/demand balance is difficult to maintain. For example, during the daytime, energy can be relatively easily generated with the use of solar panels, but the demand for energy for heating buildings and water is much higher at night. For this reason, research is required to develop effective solutions for long-term heat storage.

There are two major approaches to heat storage in the literature [26, 32, 35]. In the first approach, the heat storage system constitutes a separate device [3, 9, 23], whereas in the second approach, it is a part of an existing structure, usually a building [19, 9, 25]. Bricks [25], concrete [10, 21, 33, 36] and phase-change materials [3, 9, 29] act as heat storage materials. Heat storage materials and their parameters have been investigated in the literature [24]. These materials are used to build blocks [2, 10, 36] and walls, including flat multilayer structures [19, 26]. Heat is transferred from and to the heat storage system by a transfer medium such as water [36] or another fluid. In most systems, heat is generated by solar thermal panels [10, 23, 29].

Heat storage systems are analysed with the use of experimental, analytical and numerical methods. Numerical analyses generally rely on the Finite Difference Method [16, 31, 33]. The Finite Volume Method (FVM) is rarely applied in direct analyses of heat storage systems. It has been used to investigate heat flow through homogeneous materials in 1D and 2D space [4, 15, 20]. It was unable to find any published studies where FVM was used to analyse non-stationary heat flow through flat multilayer structures with different parameters and thickness. The hereby investigations was developed to fill this knowledge gap. The previous paper [28] focuses on the discretisation of the heat diffusion equation in 1D space for multilayer structures with different parameters and thickness. Boundary and initial conditions for numerical solutions, the so-called spanning functions for generating a numerical grid and isseues related to the time discretization were discussed. This paper is dedicated to the storage and recovery of heat from a heat storage system where water is the heat transfer medium. The article proposes an approach for using FVM to analyse heat flow through flat multilayer structures with different parameters and thickness. It should be emphasised, that the heat storage system described in the article should be treated rather as an illustration to the developed
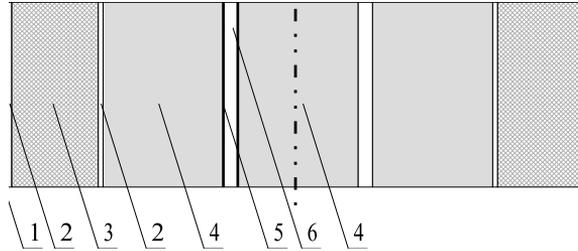
Figure 1: Modelled heat storage system

numerical code. However, the described computational system may be helpful in investigations having similar character.

2. Materials and Methods

2.1. Materials

The investigation was performed on a model wall presented in Fig. 1. Heat is stored in a block of concrete (4) separated by cavities (6) through which heat is supplied or recovered by water. Concrete is separated from water by a stainless steel plate (5). The wall is insulated with a layer of mineral wool (3) and aluminium plate (1). There are small air pockets between mineral wool and the adjacent layers (2). The wall is symmetrical, therefore, only one-half (left) of the wall was modelled by imposing the Neumann boundary condition on the axis of symmetry. The parameters of each layer were determined based on the data given by [24]. The penetration coefficient on the external surface was set at 10 $W/(m^2 \cdot K)$ [14, 30]. The parameters of each layer are presented in Tab. 1. The distribution of the diffusion coefficient $D = D(\lambda, c_p, \rho)$ (details in [28]) is presented in Fig. 2. It should be noted that the modelled wall was built for presentation purposes only, and the parameters of each layer differ considerably. This approach was adopted to verify whether the previously described algorithm [28] was implemented correctly and whether analytical procedures were smoothly executed. The author initially considered the option of relying on a configuration of multilayer walls described in the literature [13, 14, 17, 22, 30], but they were unable to find a complete and matching set of data. The undertaken experiment attempts to fill in this knowledge gap.

Table 1: Parameters in the modelled wall layers

No	Material	l	λ	c_p	ρ
		$[m]$	$[W/(m \cdot K)]$	$[J/(kg \cdot K)]$	$[kg/m^3]$
1	aluminium	0.002	220	896	2740 $[K]$
2	air	0.001	0.025	1.005	1.2
3	glass wool	0.35	0.045	840	80
4	air	0.001	0.025	1.005	1.2
5	concrete	0.5	2.75	950	2300
6	stainless steel	0.001	15	500	7900
7	water	0.05	0.6	4.18	998
8	stainless steel	0.001	15	500	7900
9	concrete	0.25	2.75	950	2300
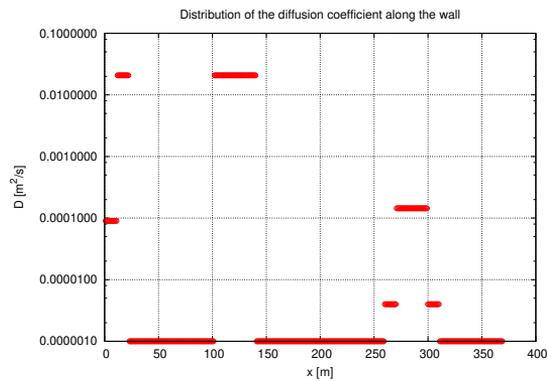
Figure 2: Diffusion coefficient in wall layers

2.2. Methods

The theoretical knowledge presented in the previous article [28] was used to develop a computer program for modelling non-stationary heat flow through flat multilayer walls with different parameters and thickness, and to analyse changes in the quantity of heat accumulated in different wall layers. The main computational module was developed in Fortran 90/95 with the use of the open-source GNU Fortran compiler [6]. The module was developed in the Gnuplot graphical environment [7] and the ParaView application for interactive visualisation [18]. The selected tools are compatible with different operating systems, in particular Windows and UNIX/Linux. A simplified algorithm of the computational module is presented in Fig. 3.

Basic information about the task (the variables were described in [28]), including the name and number of grid nodes (n^n), number of wall layers (n_l) and number of cells in each layer, was read into the program. The number of wall layers was defined, their material parameters ($\lambda_i, c_{p,i}, \rho_i$) were read, tables containing grid parameters and result tables D^n and D^c were created. The parameters were saved for nodes (index n) and cell centres (index c). This stage of programming requires information about the coordinates of all nodes (x^n) and cell centres (x^c). Data were read from a previously prepared file (the grid generator is a separate program). Node coordinates were also used to determine distances between neighbouring nodes (Δx^n) and the centres of neighbouring cells (Δx^c) in table format. Files containing the coordinates of nodes and cell centres and the corresponding values of material parameters were also created in the program. These data were used for visualisation in Gnuplot and ParaView with the use of automatically generated scripts.

Variables associated with boundary conditions, the calculation process and visualisation details are defined before the main calculation loop is executed, including the condition for ending calculations (after a given number of iterations, after a given time or when the convergence criterion has been met), type of boundary conditions (fixed or based on constant heat flux; constant or time-dependent), type of initial conditions (one constant value or table of values for different points in the grid), averaging method (harmonic or arithmetic), data save interval and other. The time step is defined, and table C is created.

The following operations are performed inside the main calculation loop:

1) table A is created (with harmonic or arithmetic means); 2) boundary conditions are imposed (fixed or based on constant heat flux; constant or time-dependent);
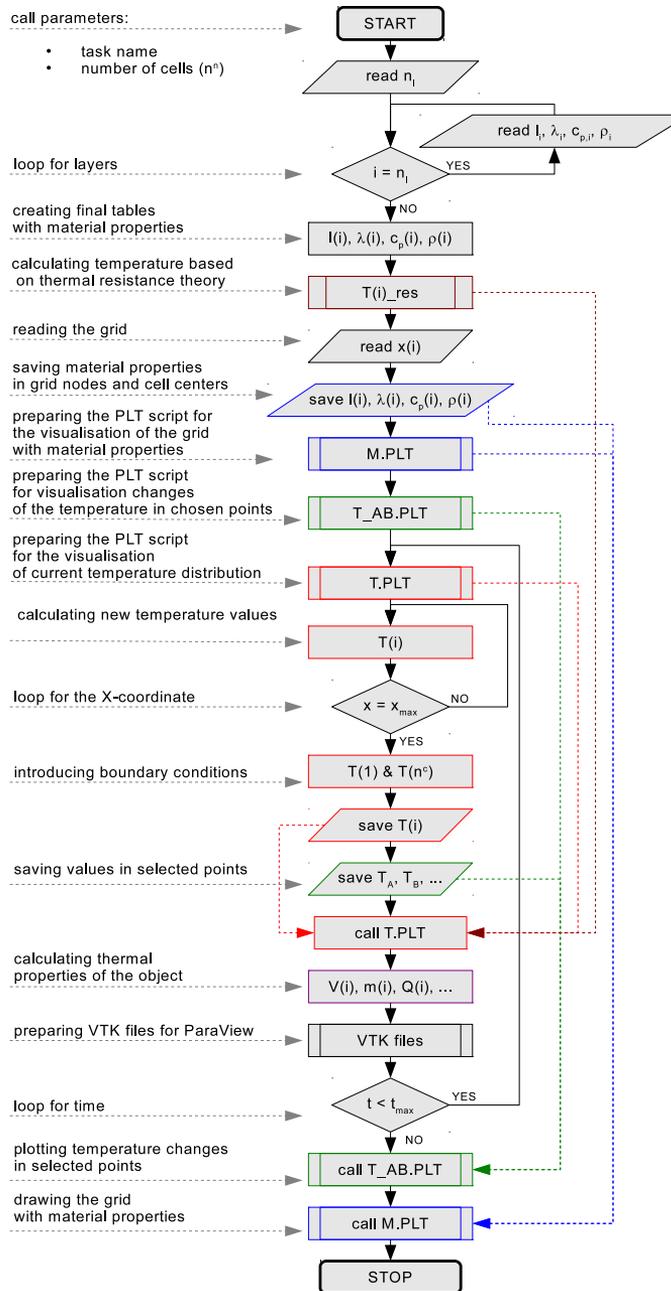
Figure 3: Simplified algorithm of the calculation module

3) table *B* is created; 4) the values from all tables are saved to file (optionally); 5) a PLT script for the current iteration is developed for visualisation [7]; 6) new temperature values are calculated for the second to the second last cell; 7) a comprehensive temperature table (with values along the boundaries) is created for visualisation; 8) the comprehensive temperature table is saved to file; 9) a PLT script for the diagram in PNG format is executed; 10) temperature values at selected points on the wall are saved (optionally); 11) accumulated heat is calculated; 12) a VTK file [37] containing information about the grid and variable values in every cell is prepared.

The system of linear equations was solved with selected direct methods (Gaussian elimination and two implementations of the Gauss-Jordan elimination method) and selected iteration methods (Jacobi method, Gauss-Seidel method, successive over-relaxation method).

The calculation program had been verified several times before the experiment by comparing simulation results with an analytical solution based on thermal resistance theory [27]. Various wall designs were used at that stage.

3. Results and Discussion

3.1. Numerical Model

The calculation grid of the proposed numerical model is presented in Fig. 4. The grid was developed with the use of spanning functions described in [28]. It is composed of 360 nodes, with the following number of nodes in each layer: 12, 12, 80, 40, 120, 12, 30, 12, 60. The total number of grid nodes is smaller by $n_l - 1$ (where n_l is the number of layers) than the total number of nodes in each layer because adjacent layers share one node. The remaining configuration parameters are presented in Tab. 2.

In the analysed wall, heat was supplied to and evacuated from the heat storage via the water-filled space in layer 7. This stage of the modelling process was conducted on the assumption that all cells in layer 7 had identical temperature at the same time and that the temperature inside cells changed over time according to any function (Fig. 5). The initial operation of the heat storage, i.e. from the moment temperature was equalised throughout the wall (including in water-filled space), was described in the model. The heat generated by the solar collector gradually (over 30 minutes) increased water temperature to around 57 [$°C$] (based on the values given by [1, 5, 12, 34]). Heat was supplied to the wall for several hours
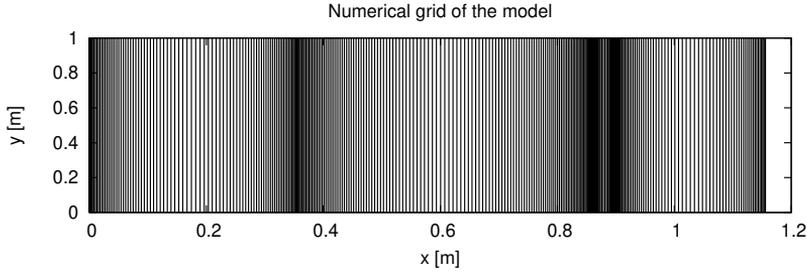
Figure 4: Visualisation of the modelled numerical grid

(6 hours in the model), after which, it was evacuated from the heat storage via a different water circuit with a temperature of 8 [$°C$]. It was assumed that the temperature of water evacuating heat from the system would not change over time. This is a certain simplification, but the magnitude of temperature increase is difficult to predict without experimental data. The modelled distribution of temperature in the wall during heat supply is presented in Fig. 6. The density of the numerical grid increases along the boundaries of each wall layer. Changes in the temperature of the heat distribution medium (layer 7) were described with the use of the following function:

$$T_7(t) = T_0, \; for \, t < 10800 [s]$$
$$T_7(t) = T_0 + 0.001(t - 10800)T_0, \; for \, t > 10800 \, and \, t < 12600 [s]$$
$$T_7(t) = T_{max}, \; for \, t > 12600 \, and \, t < 34200 [s] \qquad\qquad (1)$$
$$T_7(t) = T_{max} - 0.001(t - 34200)T_{max}, \; for \, t > 34200 \, and \, t < 35040 [s]$$
$$T_7(t) = T_{min}, \; for \, t > 35040 [s]$$

where t is time [s], and T_0, T_{max} and T_{min} are characteristic process temperatures which reached 15, 56.85 and 8 [$°C$], respectively. It should be noted that the function presented in Fig. 5 is only an example, and it can be defined with any set of values and time steps.

The temperature profile of the wall at different time steps is presented in Fig. 7. The first diagram corresponds to the period when heat was not exchanged by the transfer medium (water). The temperature of the wall increased slowly when heat was supplied to the left side of the wall. The second diagram presents the temperature profile of the wall immediately before the heat source was activated in layer 7. The following two diagrams correspond to the beginning and end of the period marked by an increase in temperature. The Neumann condition imposed on

Table 2: Parameters in the modelled wall layers

Number of grid nodes/cells	360
Precision	double
Boundary condition on the left side	mixed
Temperature on the left side	25.0 [$°C$]
Heat transfer coefficient on the left side	10 [$W/m^2 \cdot K$]
Boundary condition on the right side	Neumann
Determination of initial temperature	based on constant value
Initial wall temperature	15 [$°C$]
Global diffusion coefficient formula	$D = \lambda/(c_p \cdot \rho)$
Averaging method for diffusion coefficient	weighted harmonic mean
Heat calculation method	relative to constant value
Reference temper. for calculating heat transfer	0 [$°C$]
Side length of wall layer	1.0 [m]
Time-stepping method	Crank-Nicolson (implicit)
Time step	0.1 [s]
Maximum computing time	86400 [s] (24 [h])
Method of solving a system of equations	Gauss-Jordan
Temperature convergence criterion	not used
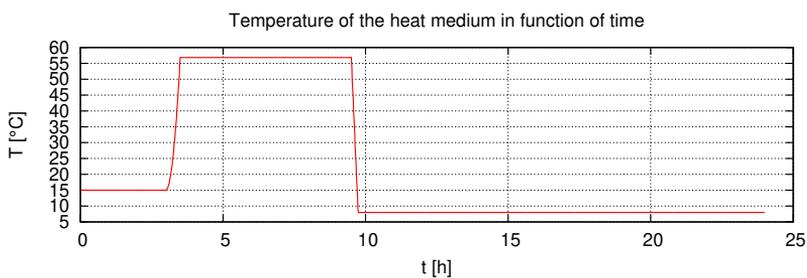
Figure 5: Distribution of changes in the temperature of the heat medium over time
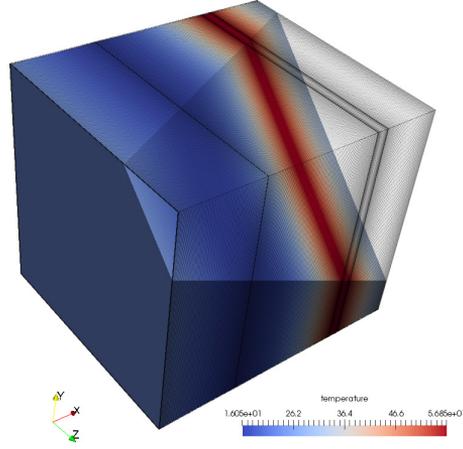
Figure 6: Visualisation of the temperature profile inside the wall during heat supply

the system's axis of symmetry meets the present criteria. The last two diagrams correspond to the period when heat was evacuated from the system by water with lower temperature. In the last diagram, heat was nearly entirely evacuated from the system. An analysis of the temperature profile indicates that the central part of the wall (separated by the line of symmetry) could be thinner. In the presented cycle, the central part of the wall is not heated to the maximum temperature (temperature of water supplying heat) or cooled to the minimum temperature (temperature of water evacuating heat) in its entirety. The above indicates that wall thickness and the parameters of each layer can be optimized in the developed program. However, experimental data need to be gathered before the practical applicability of the discussed calculation model can be postulated.

The quantity of heat accumulated in the material (every grid cell) at any time step can be calculated based on the temperature inside grid cells:

$$Q_i^{t,c} = m_i c_{p,i}^c (T_i^{t,c} - T_{i,ref}^c) \tag{2}$$

or

$$Q_i^{t,c} = \rho_i^c V_i c_{p,i}^c (T_i^{t,c} - T_{i,ref}^c) = \rho_i^c S \Delta x_i^n (T_i^{t,c} - T_{i,ref}^c), \tag{3}$$

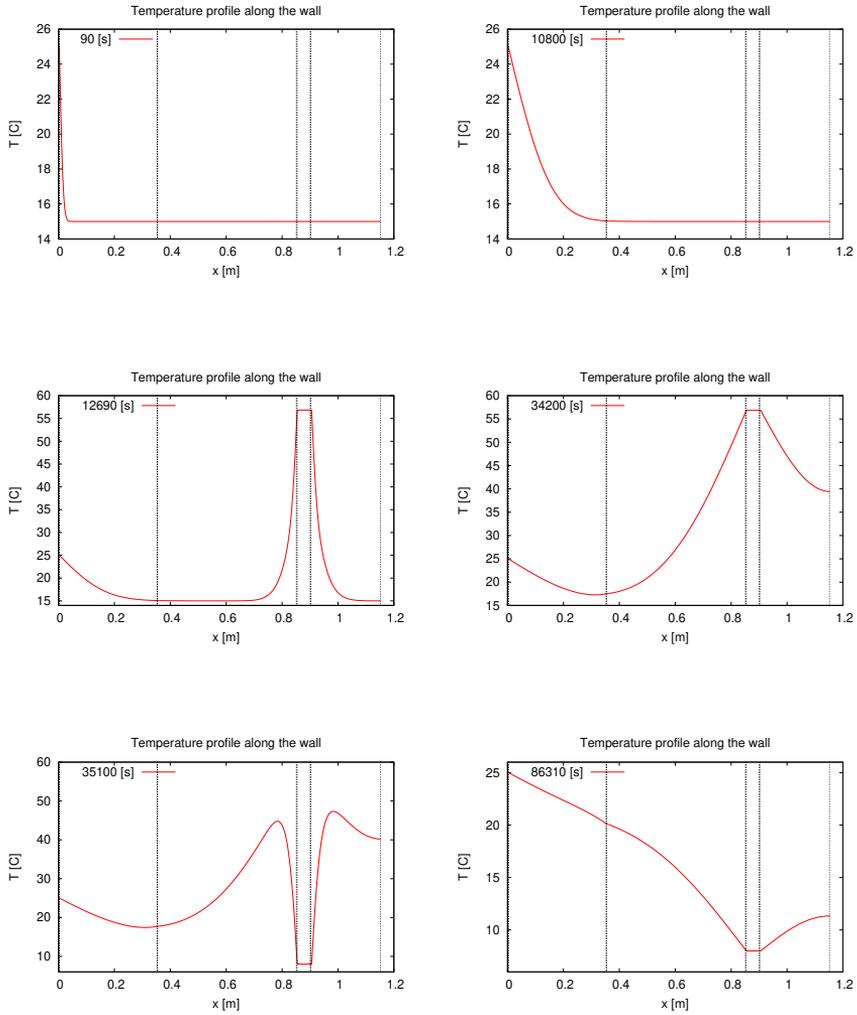where: $Q_i^{c,t}$ - heat accumulated in the ith cell [J], m_i - mass of the ith cell [kg],

Figure 7: Visualisation of the temperature along the wall at selected time steps

$c_{p,i}^c$ - specific heat of the material inside the ith cell [$J/(kg \cdot K)$], $T_i^{c,t}$ - temperature of the ith cell [K] in time t [s], $T_{i,ref}^c$ - reference temperature for calculating heat [K], ρ_i^c - density of the material in the ith cell [kg/m^3], V_i - volume of the ith cell [m^3], S - wall area perpendicular to heat flow [m^2], Δx_i^n - thickness of the ith cell (distance between nodes limiting the ith cell) [m]. Reference temperature $T_{i,ref}^c$ can be defined as initial wall temperature in any cell or any other common value for all cells. In the presented model, reference temperature was 0 [$°C$].

Total heat accumulated in the ith cell of the grid was calculated with the use of formula (2). However, cells differ in length, therefore, specific heat, rather than total heat, should be calculated in reference to cell mass in certain situations, for example when visualising heat distribution along the wall. The above approach ensures that the diagram is not distorted by uneven distribution of points on the x-axis (Fig. 8):

$$q_i^{t,c} = \frac{m_i c_{p,i}^c (T_i^{t,c} - T_{i,ref}^c)}{m_i} = c_{p,i}^c (T_i^{t,c} - T_{i,ref}^c). \tag{4}$$

where: q - specific heat [J/kg].

The direction of changes in heat distribution over time can be defined in every grid cell based on the plus or minus sign in two neighbouring time steps:

$$dQ_i^{\Delta t,c} = Q_i^{t+\Delta t,c} - Q_i^{t,c}. \tag{5}$$

A plus sign indicates that heat is accumulated in the cell, whereas a minus sign indicates that heat is evacuated from the cell (Fig. 9). The reference temperature is not taken into account in heat calculations.

Local increases in heat accumulation can be summed up for the entire grid to determine whether heat is being accumulated or evacuated from the system (wall):

$$dQ_{sum} = \sum_{i=1}^{M} dQ_i^{\Delta t,c}. \tag{6}$$

The corresponding information is presented in Fig. 10. The greatest local differences in heat distribution are observed at the beginning of the calculation process (several dozen first iterations) in the initial stage of solving the diffusion equation. These differences result from large temperature gradients in the numerical grid. Similar gradients appear later when the temperature of the heat medium changes. Two distinct peaks can be observed: a positive peak (heat is supplied by
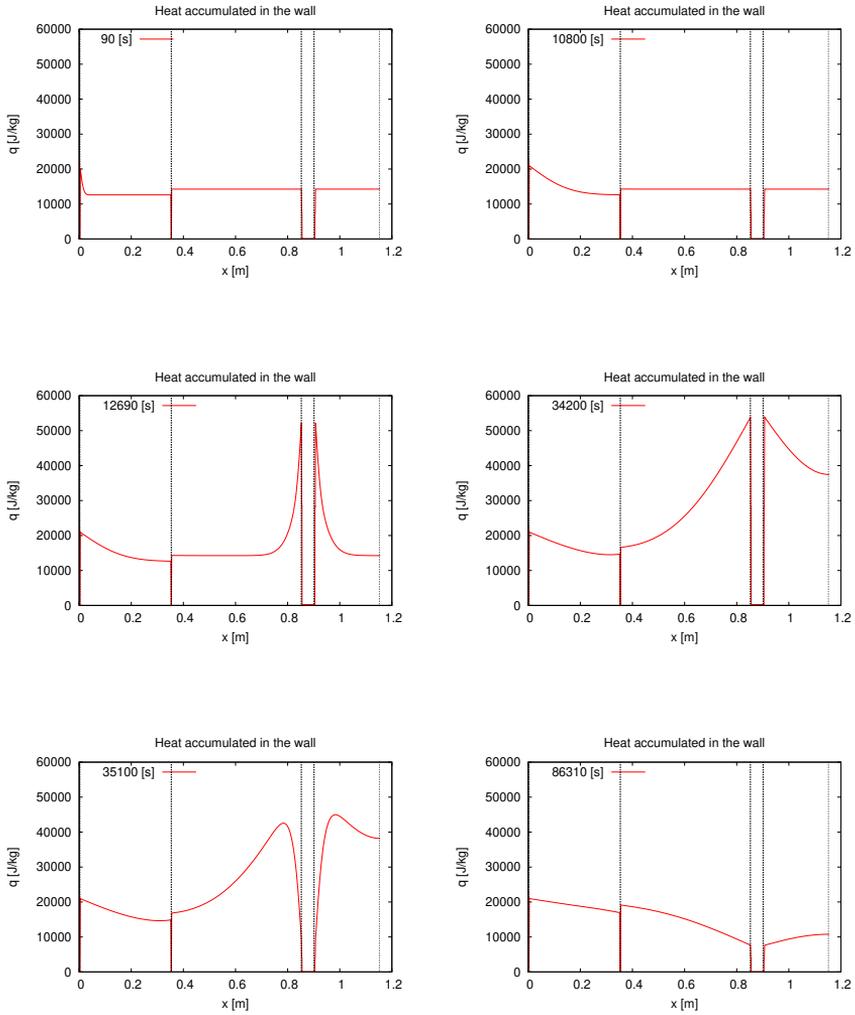
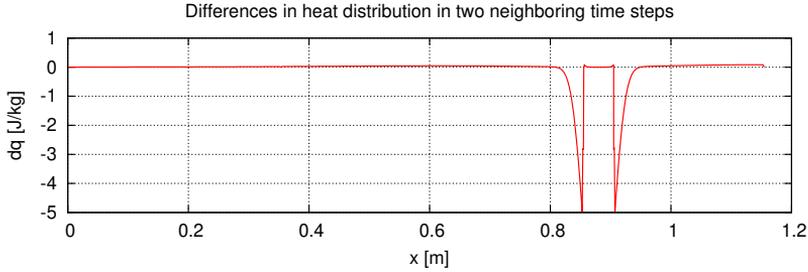Figure 8: Heat accumulated in the wall at different time steps

Figure 9: Visualisation of changes in heat distribution in the wall in two neigh-bouring time steps in the initial stage of heat evacuation
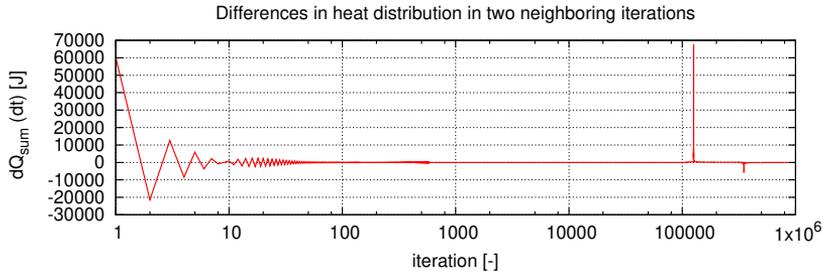

Figure 10: Total changes in heat distribution over time (as a function of iteration)

the heat medium) and a negative peak (heat is evacuated by the heat medium). Peak size is determined by temperature.

The convergence of the performed calculations can be approximated to track non-stationary heat transfer. Convergence is defined as the total temperature increase in all grid cells, calculated for two neighbouring time steps:

$$\left| \sum_{i=2}^{M-1} (T_i^{t+\Delta t} - T_i^t) \right| = \left| I_C \right| < \delta, \tag{7}$$

where I_C is the convergence coefficient, and δ is the convergence criterion which, when met, ends the program (this option was not used in our simulation). As expected, the periods marked by changes in the temperature of the heat medium were the most non-stationary stages of the process.
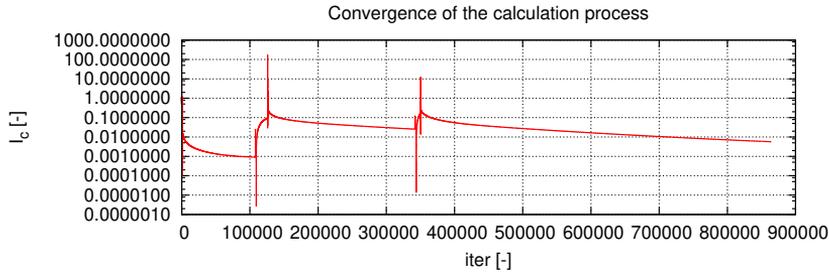
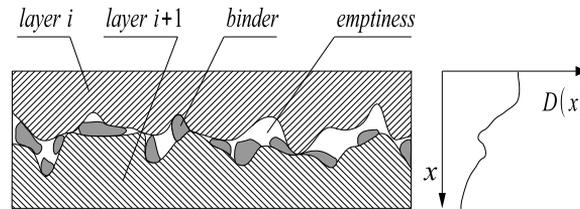Figure 11: Changes in the convergence coefficient

Figure 12: The concept taking into account contact resistance by modification of the material parameter

3.2. Development possibilities of the numerical code

An interesting issue related to heat flow through multilayer structures is the problem of thermal resistance present at the interface of individual layers [8, 11, 31]. The literature usually introduces contact models with various degrees of complexity. In this paper, a different approach is proposed (Fig. 12), involving a local change of material parameters (see table $D = D(t, x)$). Such a change can be introduced in a different manner for every layer contact surface, and can describe the existence of both voids (e.g. air pockets) and filling with different material (e.g. adhesive, mortar, plaster, etc.). It is important, in the case of parameter modification at the layer interface area, that the numerical grid be sufficiently dense. In the case of one-dimensional flow through a structure with a specified area (e.g. unitary), the best solution should be to introduce weighted averages. Note that the concept described in relation to one-dimensional heat flows may lead to considerable simplification.

The source term of the thermal diffusion equation can be used to include a few more phenomena and processes. Among them are phase transitions which lead to

the difference between the heat exchanged through the adjacent body area (e.g. layers). This difference results from the so called latent heat. Fig. 13 indicates an example of temperature distribution in a three-layer structure, in which the middle layer can be subject to phase transitions. Assuming that melting occurs in that layer, less heat will diffuse to the outer layer than in the absence of melting, and the entire temperature distribution will move downward (T' represents temperature distribution for the melting option). In the case of freezing, the process will be identical, except that the temperature distribution will move upwards, since the latent heat is dissipated outside.
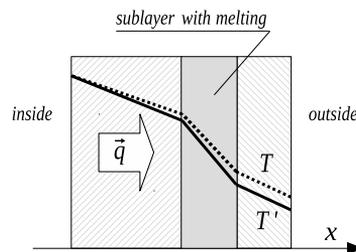
Figure 13: Schematic presentation of heat sources behaviour during phase transition of a single layer

The source component can be used to describe systems in which the material contains an additional component, e.g. humidity. It can also be subject to phase transitions affecting the energy balance of the entire structure (Fig. 14). If this is the case, moisture evaporation from the structure and its freezing can both be considered. Such phenomena can be significant in external layers exposed to variable thermodynamic conditions. It is important that the source intensity depends on a momentary change of moisture content, so it has to be described by the application of an additional model taking into account the time factor.

Another factor that can be described with the aid of the source s_T is heat exchange due to advection in the expansion joint layer (Fig. 15). A basic version of this phenomenon was applied in the paper. A complete model of the system should include fluid transport in that layer. However, the expansion joint layer can be considered, with some approximation, as the heat exchange zone, particularly when the process is of a stationary nature. It may be somehow difficult to determine the intensity of the source, in particular if the flow in that layer is turbulent. Accurate calibration of the source may require proper experiments to be carried out.
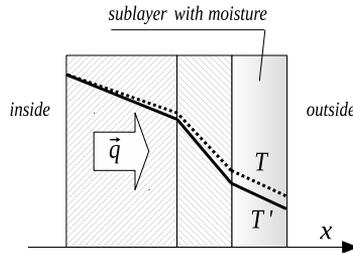
Figure 14: Schematic presentation of heat sources behaviour during phase transition due to the evaporation of moisture contained in the material
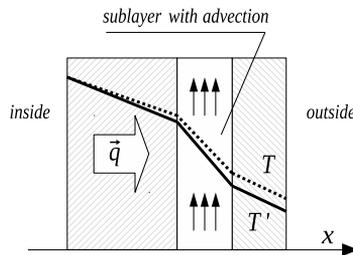

Figure 15: Schematic presentation of heat source behaviour due to advection in the expansion joint layer

One more factor that can be considered through an appropriate description of the source component is biochemical activity. It may cause widespread or local temperature differences affecting the energy balance of the structure. Fig. 16 provides a schematic presentation of activity causing local heat release in a given structure layer, resulting in lifting the temperature distribution curve.

The source component can also be used to describe the radiation phenomenon (Fig. 17). If this is the case, temperature change in material depends on whether the outer surface of the structure releases or absorbs heat. It is worth adding that the radiation effect can also be considered by the proper modification of the boundary conditions.

Considering the above deliberations, it can be stated that, in a general case, the source component of the thermal diffusion equation should take the form:

$$s_T = s_T^{latent\,heat} + s_T^{moisture} + s_T^{contact} + s_T^{advection} + s_T^{biochemica} + s_T^{radiation} + ... \quad (8)$$
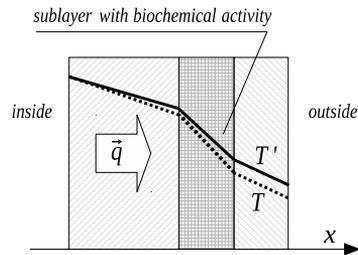
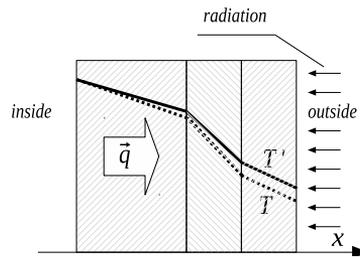Figure 16: Schematic presentation of the action of biochemical heat sources

Figure 17: Schematic presentation of the behaviour of radiation heat source

Determination of the factors to be left out and models to be adopted for the remaining components depends on the specific case.

4. Summary

The results of this study support the formulation of the following conclusions:

1. Individual components of the computational algorithm, including numerical solutions for the heat diffusion equation, weighted (harmonic or arithmetic) averaging of material parameters and the spanning function theory, have been previously described separately in the literature. However, in this study, the above components were combined to develop a useful tool for analysing changes in heat distribution in multilayer walls.

2. This study proposes the use of the finite volume method for solving heat diffusion equations. Such approach makes a direct reference to the laws of physics and creates new possibilities for analysing heat transfer.

3. In the developed program, the tools for tracking changes in heat distribution

in sublayers forming a flat wall are proposed. At the present stage of research, these tools are sufficient for comparing the extent and rate of changes in energy accumulated in various configurations of multilayer walls.

4. The developed computational module is highly flexible and open to modification. Most importantly, all variables in the program can be functions of space and time, and they can be freely correlated.

5. It is possible to consider a number of additional physical, chemical and biological factors by the proper use of the source component and diffusion equation.

6. The developed program runs much faster in UNIX/Linux operating systems than in the Windows environment. The program was originally written in the Unix environment, and the transfer to the Windows environment compromised its operating speed. The above underlines the importance of universal numerical codes that can be applied in different operating systems.

7. The main advantage of the proposed approach is that it supports full control over all computational processes.

References

[1] Ayompe L.M., Duffy A., *Thermal performance analysis of a solar water heating system with heat pipe evacuated tube collector using data from a field trial*, Solar Energy, Vol. 90, 2013, 17-28.

[2] Bergan P.G., Greiner C.J., *A new type of large scale thermal energy storage*, Energy Procedia, Vol. 58, 2014, 152-159.

[3] Boonsu R., Sukchai S., Hemavibool S., Somkun S., *Performance Analysis of Thermal Energy Storage Prototype in Thailand*, Journal of Clean Energy Technologies, Vol. 4(2), 2016, 101-106.

[4] Després B., *Non-linear schemes for the heat equation in 1D*, ESAIM: Mathematical Modelling and Numerical Analysis, Vol. 48(1), 2014, 107-134.

[5] Faiman D, Hazan H., Laufer I., *Reducing the heat loss at night from solar water heaters of the integrated collector-storage variety*, Vol. 71(2), 2001, 87-93.

[6] GNU Fortran Home Page [on-line]. URL: https://gcc.gnu.org/fortran/ (Available at May 4, 2017).

[7] Gnuplot Home Page [on-line]. URL: http://www.gnuplot.info/ (Available at May 4, 2017).

[8] Hong-Bo W., *Heat transfer analysis of components of construction exposed to fire*, PhD Thesis, Department of Civil Engineering and Construction, University of Salford, Manchester, M5 4VVT, England 1005.

[9] Laing D., Bauer T., Steinmann, W.-D., Lehmann D., *Advanced high temperature latent heat storage system - design and test results*, The 11th International Conference on Thermal Energy Storage, Effstock 14-17 June 2009, Stockholm, Sweden.

[10] Laing D., Lehmann D., *Concrete storage for solar thermal power plants and industrial process heat*, IRES III 2008, 3rd International Renewable Energy Storage Conference, 24.-25.11.2008, Berlin.

[11] Lienhard J. H. IV, Lienhard J. H. V., *A heat transfer textbook*, Cambridge, Massachusetts, 2001.

[12] Liu Y-M., Chung K-M, Chang K-C., Lee T-S., *Performance of Thermosyphon Solar Water Heaters in Series*, Energies, Vol. 5, 2012, 3266-3278.

[13] Martin K., Escudero C., Erkoreka A., Flores I., Sala J.M., *Equivalent wall method for dynamic characterisation of thermal bridges*, Energy and Buildings, Vol. 55, 2012, 704-714.

[14] Mierzwiczak M., *Steady-state heat conduction in multilayered plate with temperature-dependent thermal conductivity* (in Polish), Scientific papers of Poznan University of Technology, Vol. 9 (2008), 67-79.

[15] Nance D.V., *Finite volume algorithms for heat conduction*, Air Force Research Laboratory, Technical Report for period December 2009 - May 2010. AFRL-RW-EG-TR-2010-049.

[16] Nikitin V., Lapko A., *On modelling heat and moisture transfer in sandwich wall and slab structures*, Journal of Civil Engineering and Management, Vol. 12(4), 2006, 337-343.

[17] Niu F., Yu Y., *Location and optimization analysis of capillary tube network embedded in active tuning building wall*, Energy, Vol. 97, 2016, 36-45.

[18] ParaView Home Page [on-line]. URL: http://www.paraview.org/ (Available at May 4, 2017).

[19] Pasupathy A., Velraj R., *Phase Change Material Based Thermal Storage for Energy Conservation in Building Architecture* International Energy Journal, Vol. 7(2), 2006, 147-159.

[20] Patil P., Prasad J.S.V.R.K., *The unsteady state finite volume numerical grid technique for multidimensional problems*, International journal of advances in applied mathematics and mechanics, Vol. 2(2), 2014, 78-87.

[21] Pomianowski M., Heiselberg P., Jensen R.L., *Dynamic heat storage and cooling capacity of a concrete deck with PCM and thermally activated building system*, Energy and Buildings, Vol. 53, 2012, 96-107.

[22] Ramin H., Hanafizadeh P, AkhavanBehabadi M.A., *Comparative study between dynamic transient and degree-hours methods to estimate heating and cooling loads of building's wall*, JCAMECH, Vol. 46(2), 2015, 135-165.

[23] Reddy R.M., Nallusamy N., Reddy K.H., *Experimental Studies on Phase Change Material-Based Thermal Energy Storage System for SolarWater Heating Applications*, Ashdin Publishing Journal of Fundamentals of Renewable Energy and Applications, Vol. 2, 2012, ID R120314, 6 p.

[24] Rempel A. R., Rempel A. W.: Rocks, Clays, Water, and Salts, *Highly Durable, Infinitely Rechargeable, Eminently Controllable Thermal Batteries for Buildings*, Geosciences, Vol. 3 (2013), 63-101.

[25] Sala J.M., Urresti A., Martin K., Flores I., Apaolaza A., *Static and dynamic thermal characterisation of a hollow brick wall: Tests and numerical analysis*, Energy and Buildings, Vol. 40(8), 2008, 1513-1520.

[26] Sharma A., Tyagi V.V., Chen C.R., Buddhi D., *Review on thermal energy storage with phase change materials and applications*, Renewable and Sustainable Energy Reviews, Vol. 13(2), 2009, 318-345.

[27] Sobieski W., *Thermodynamics in experiments* (in Polish) [on-line]. URL: http://pracownicy.uwm.edu.pl/wojsob/ (Available at March 8, 2017), Olsztyn, 2012.

[28] Sobieski W., Trykozko A., *Discretisation of a thermal diffusion equation in multilayer structures with variable material parameters and different thicknesses* (submitted).

[29] Szymocha K., *Advanced thermal solar system with heat storage for residential house space heating*, SESCI 2005 Conference British Columbia Institute of Technology, Burnaby, British Columbia, Canada, August 20-24, 2005.

[30] Tamene Y., *Numerical and Economical Study of Thermal Insulation in Multilayer Wall Exposed to Real Climatic Conditions*, Athens Journal of Technology Engineering, Vol. 1(2), (2014), 137-148.

[31] Tamene Y., Bougriou C., Bessah R., *Thermal behaviour of a multilayer media in transient regime* Revue des Energies Renouvelables, Vol. 10(3), 2007, 397-405.

[32] Tyagi V.V., Buddhi D., *PCM thermal storage in buildings: A state of art*, Renewable and Sustainable Energy Reviews, Vol. 11, 2007, 1146-1166.

[33] Wongpanyo W., Charoensawan P., Rakwichian W., Seetapand P., *Improving Heat Transfer Performance of Concrete Thermal Energy Storage with Use of Local Material*, International Journal of Renewable Energy, Vol. 3(2), 2008, 15-26.

[34] Zelzouli K., Guizani A., Sebai R., Kerkeni C., *Solar Thermal Systems Performances versus Flat Plate Solar Collectors Connected in Series*, Engineering, Vol. 4(12), 2012, 881-893.

[35] Zhang Y., Zhou G., Lin K., Zhang Q, Di H., *Application of latent heat thermal energy storage in buildings: State-of-the-art and outlook*, Building and Environment, Vol. 42, 2007, 2197-2209.

[36] Valentina A. S., Carmelo E. M., Giuseppe M. G., Rosa Di Maggio, Fabrizio G., Domenico M., Marco L., *Application of Solar Energy*, chapter 6 "Conceptual Study of a Thermal Storage Module for Solar Power Plants with Parabolic Trough Concentrators". INTECH, 2013.

[37] Visualization Toolkit [on-line]. URL: http://www.vtk.org/ (Available at May 4, 2017).

INSTRUCTION FOR AUTHORS

Journal of Applied Computer Science publishes original papers only. Full papers not exceeding 22 standard pages (30 lines × 60 characters), should be submitted electronically, or on CD/DVD. They will not be returned except for editorial reasons.

Contributions should be written in good English and prepared in LaTeX. The abstract should not contain any formulas or references, and should not exceed 200 words. The Authors are required to follow the LaTeX `jacsart.cls` and BiBTeX `aiaa-jacs.bst` templates and styles available at: `http://www.jacs.it.p.lodz.pl` (as .ZIP file).

Illustrations (with captions), drawings, tables, diagrams and equations should be incorporated in the text and numbered consecutively. Mathematical symbols should be typeset using the math mode of LaTeX. The references should be enumerated in order of appearing in text, and formatted using the BiBTeX program and the `aiaa-jacs.bst` style available at: `http://www.jacs.it.p.lodz.pl` (as .ZIP file).

COPYRIGHT

AIMS AND SCOPE

Journal of Applied Computer Science publishes original papers concerning theory and practice of computer science and innovative computer technology as well as their application in engineering, biomedicine, ecology, socioeconomics and education. It is the place for exchange of information and research results within the following scope:

- Machine intelligence and soft-computing with particular emphasis on
  - neural networks, fuzzy systems and evolutionary algorithms;
  - expert, agents, diagnostic and decision supporting systems;
  - data mining and warehousing;
  - reasoning, knowledge extraction and information management.
- Applications of computer science in modeling, simulation, identification and control.
- Image processing and pattern recognition.
- Computer graphics, visualization and multimedia.
- Databases and information systems.
- Computer security and recovery.
- Communication, internet and distributed computer systems.
- Software engineering and tools.

The book reviews and conference announcements are also welcome.